Coastal Circulations

Topics:

1. Tides
2. Storm Surges
3. Subtropical Eastern Boundary Upwelling Systems
4. Coastally Trapped Waves
5. Shelf-Break and Tidal-Mixing Fronts
6. Wave-Driven Littoral (Beach) Currents
7. Estuarine Circulations & their Reverse
8. Coastal Biogeochemistry

.

Concept: Shallow water regions next to coasts have distinctive physical and biogeochemical behaviors compared to deeper water.

Tidal currents, storm surges, and tsunamis amplify in shallow, constricted bays.

Surface gravity waves break in the littoral zone (< 10 m depth)

Rivers enter the ocean carrying buoyancy (fresh water) and chemical loads ($e.g.$, from agricultural run-off, a prevalent cause of coastal hypoxia, as off the Mississippi or Yangtze Rivers).

Topography comes to the surface, the bottom boundary layer affects even surface currents, and the slope supports boundary currents and topographic waves.

Many species use shallow water for spawning.

Fishing pressures $\longrightarrow$ over-fishing is particularly prevalent along coasts.

Tides

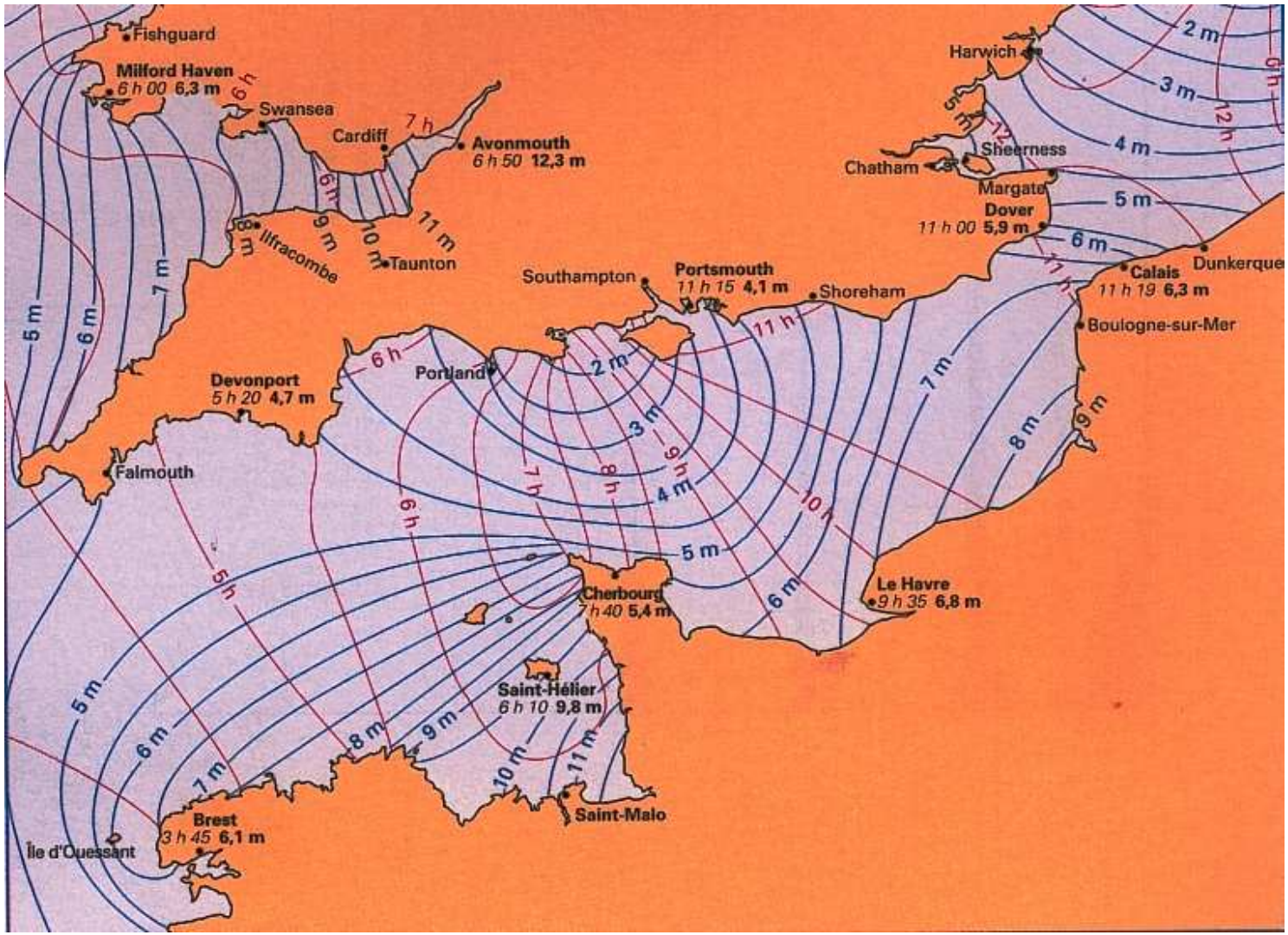

Barotropic Tides: regional sea level amplitude [m] (peak-to-trough) and phase [hours in a cycle] of the M2 (lunar semi-diurnal) tide around the English Channel determined mainly from coastal tide gauges (SHOM, 1997). (A repeated figure.) Tidal height and current amplify in shallow water, and baroclinic (internal-wave) tides are also preferentially generated there by barotropic tidal flow over topography in stratified water. [See Chap. 17 of Stewart (2008) for more about tides and coastal currents.]

Storm Surges

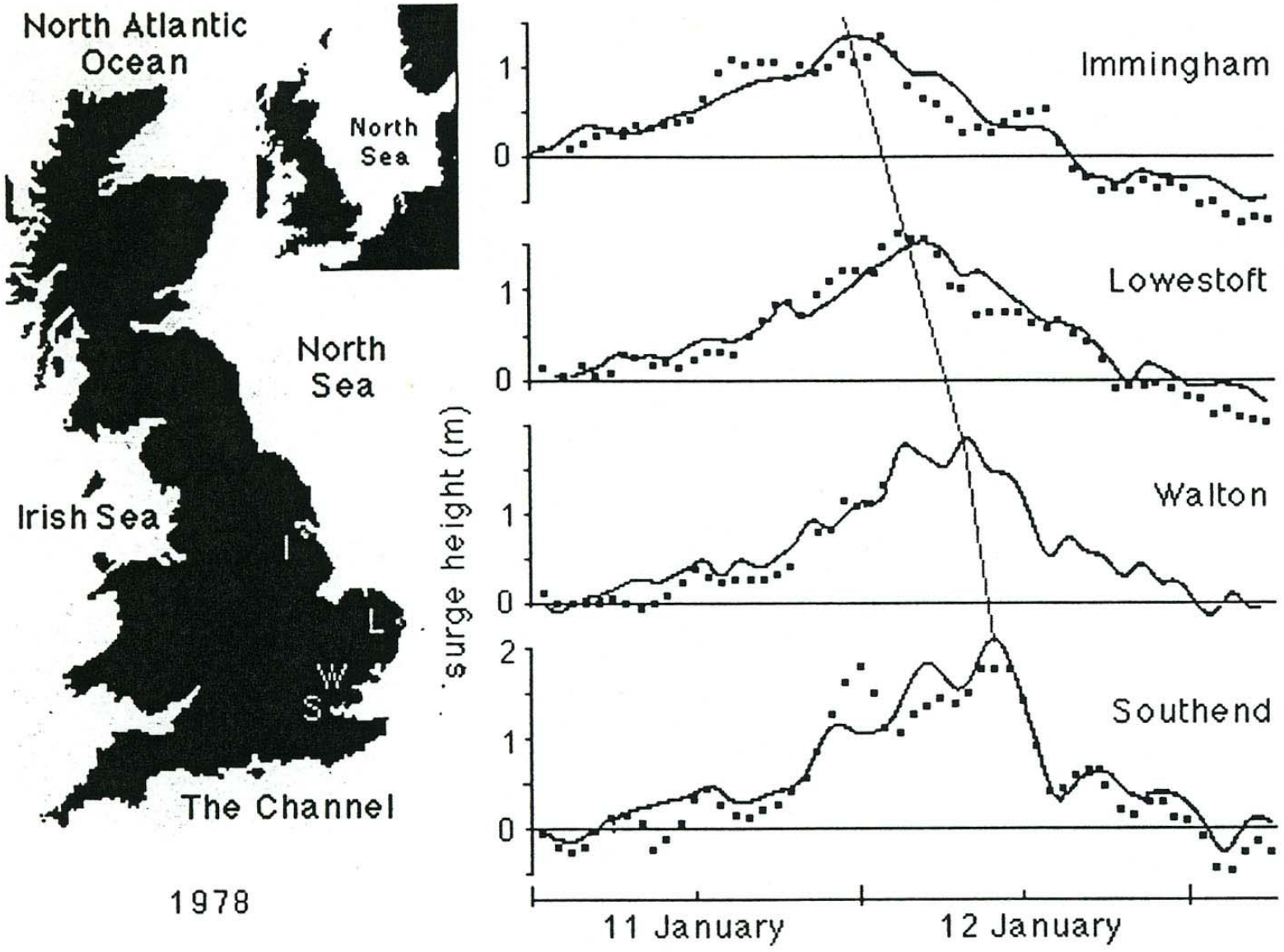

A storm surge anomaly along the east coast of England (tide subtracted). This occurs with the conjunction of high tide and wind-induced currents that propagate as a shallow water gravity wave. (Tomczak, 1998)

Subtropical Eastern Boundary Upwelling Systems

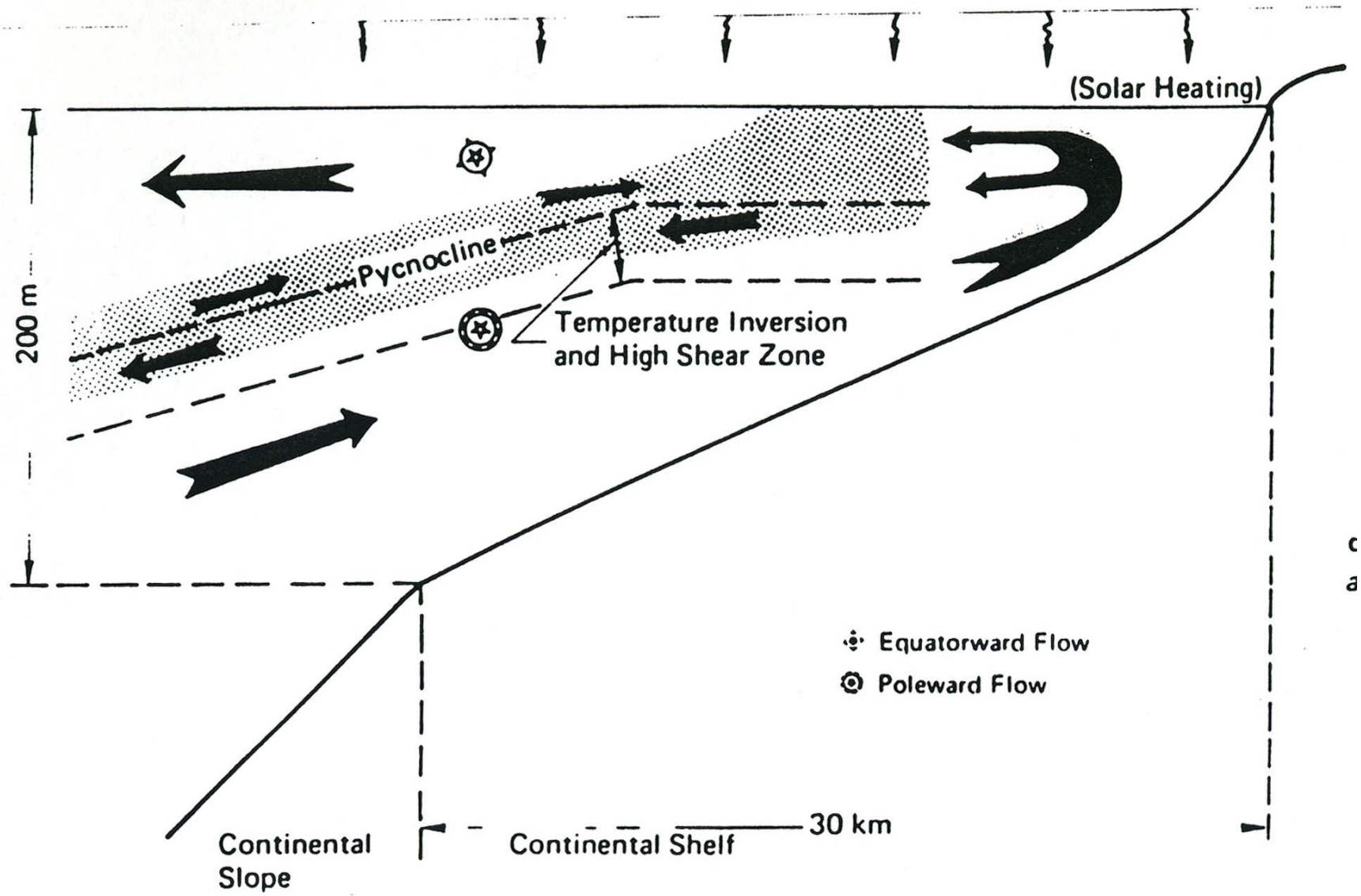

Sketch of upwelling circulation adjacent to an eastern boundary with equatorward winds. Note the Ekman zonal overturning circulation, pycnocline uplift, and vertically sheared alongshore flow, including a poleward Undercurrent in the pycnocline. Substropical eastern boundaries have highly productive ecosystems and fisheries (NW&SW Africa, California, Peru-Chile). (O'Brien, 1975)

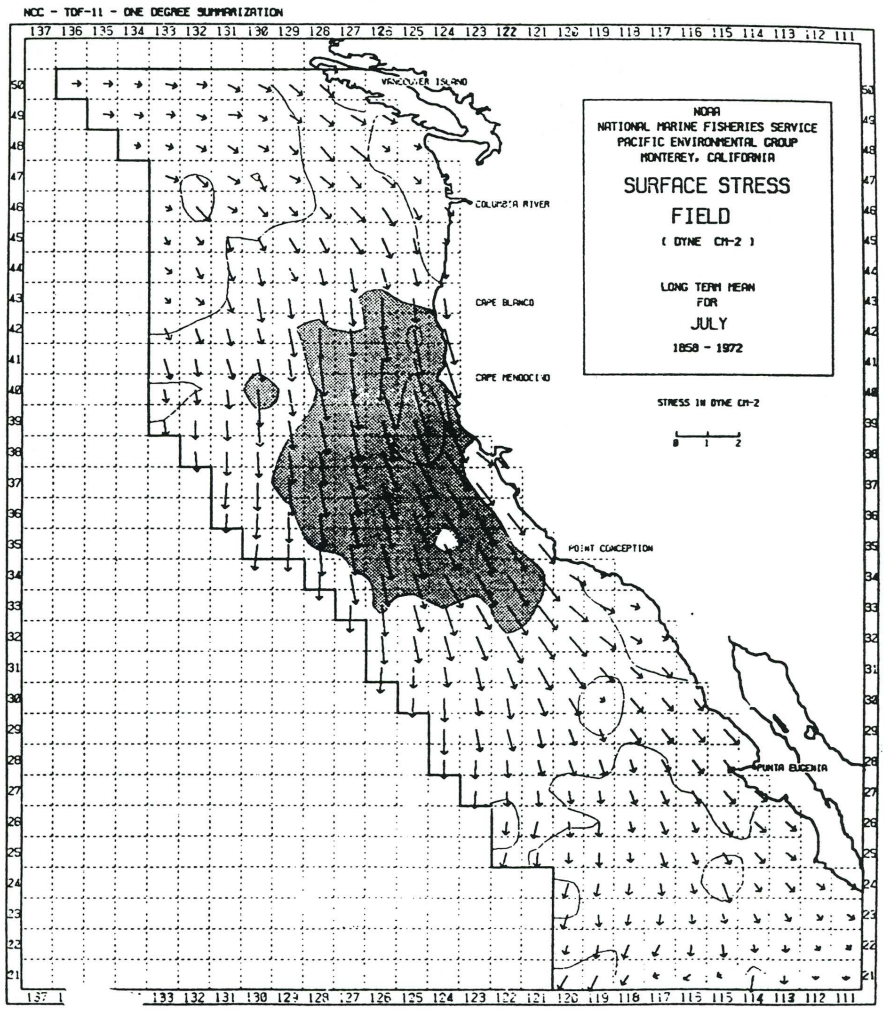

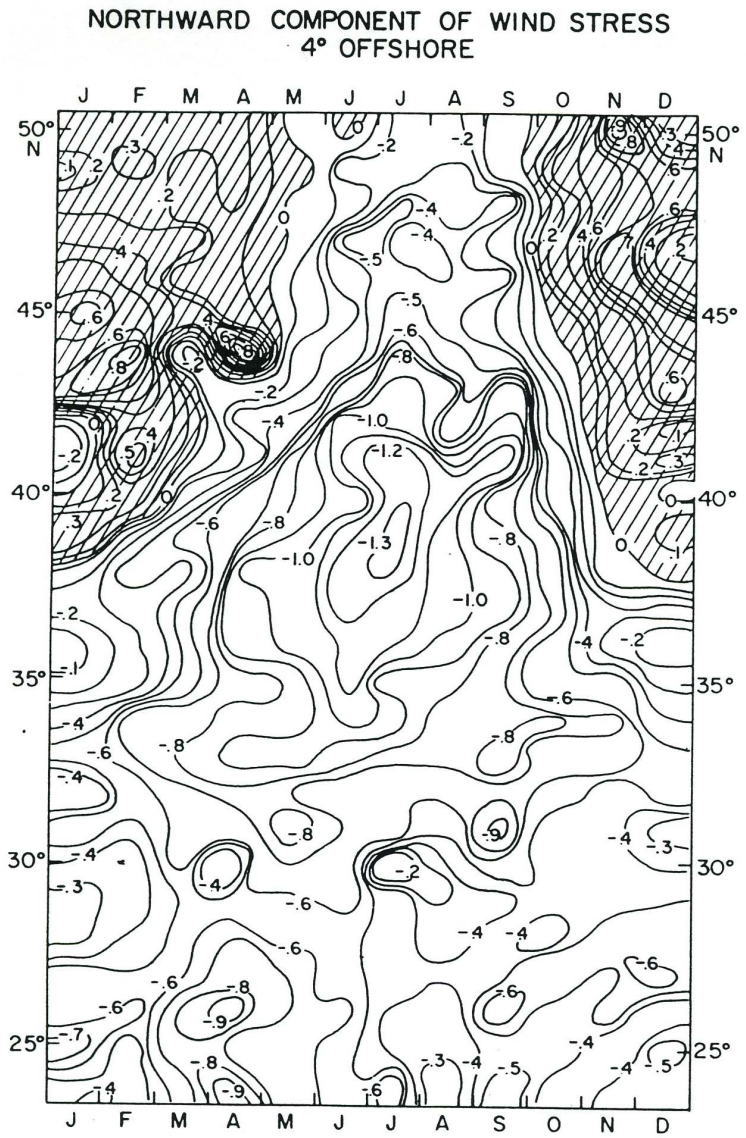

(a) Summer winds and (b) seasonal cycle of winds off the U.S. West Coast. The winds are generally equatorward except for passing storms and are strongest in the summertime; hence the upwelling and alongshore currents are strongest then as well. Upwelling becomes seasonal north of 40^{o}N, $i.e.$, the CA-OR border. (Hickey, 1979)

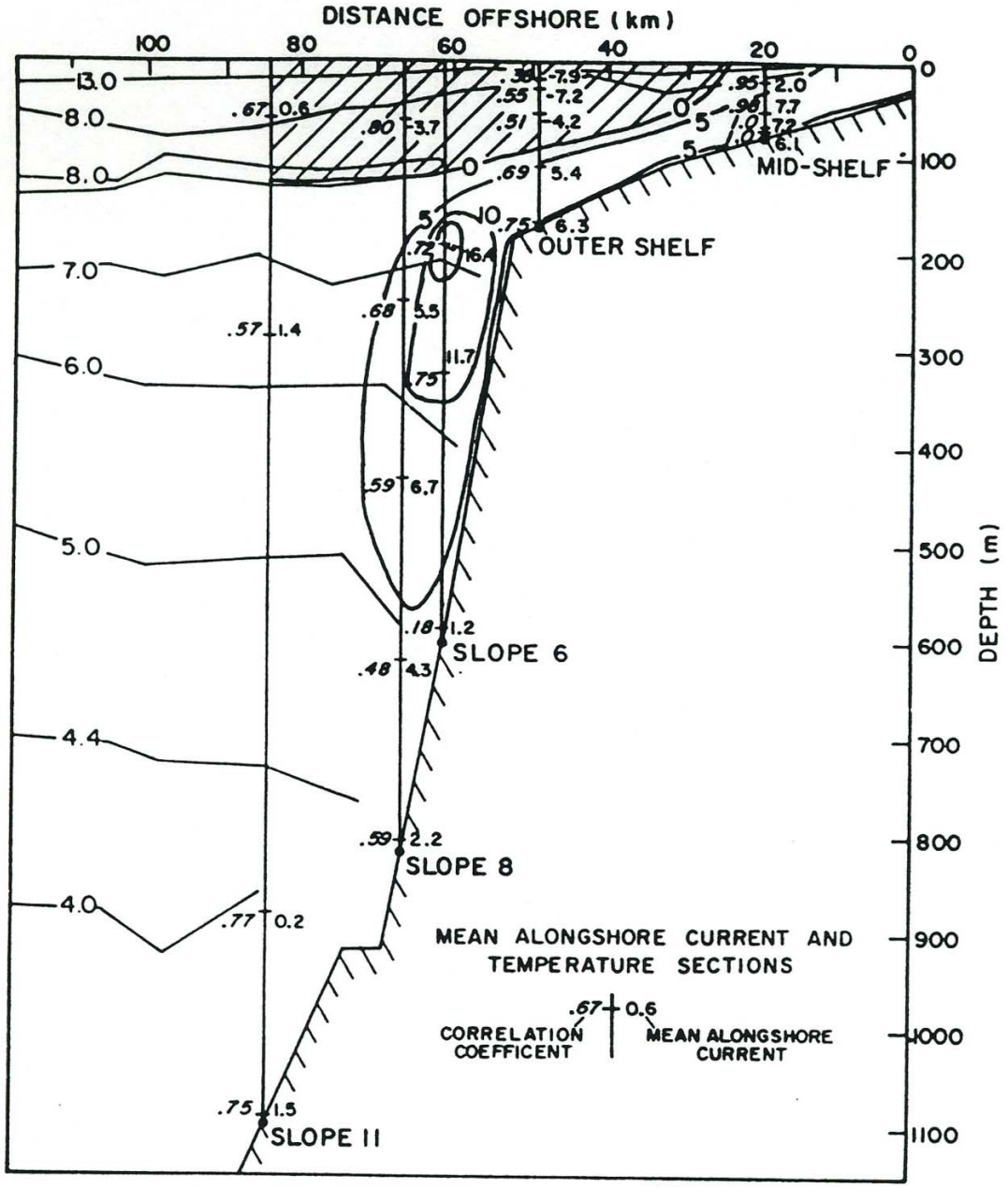

Along-shore currents off the U.S. West Coast. The broad equatorward current at the surface is called the California Current, and the poleward flow on the continental slope is the California Undercurrent. The lateral lines are isotherms [C], and the velocity unit is cm s^{-1}. (Hickey, 1979)

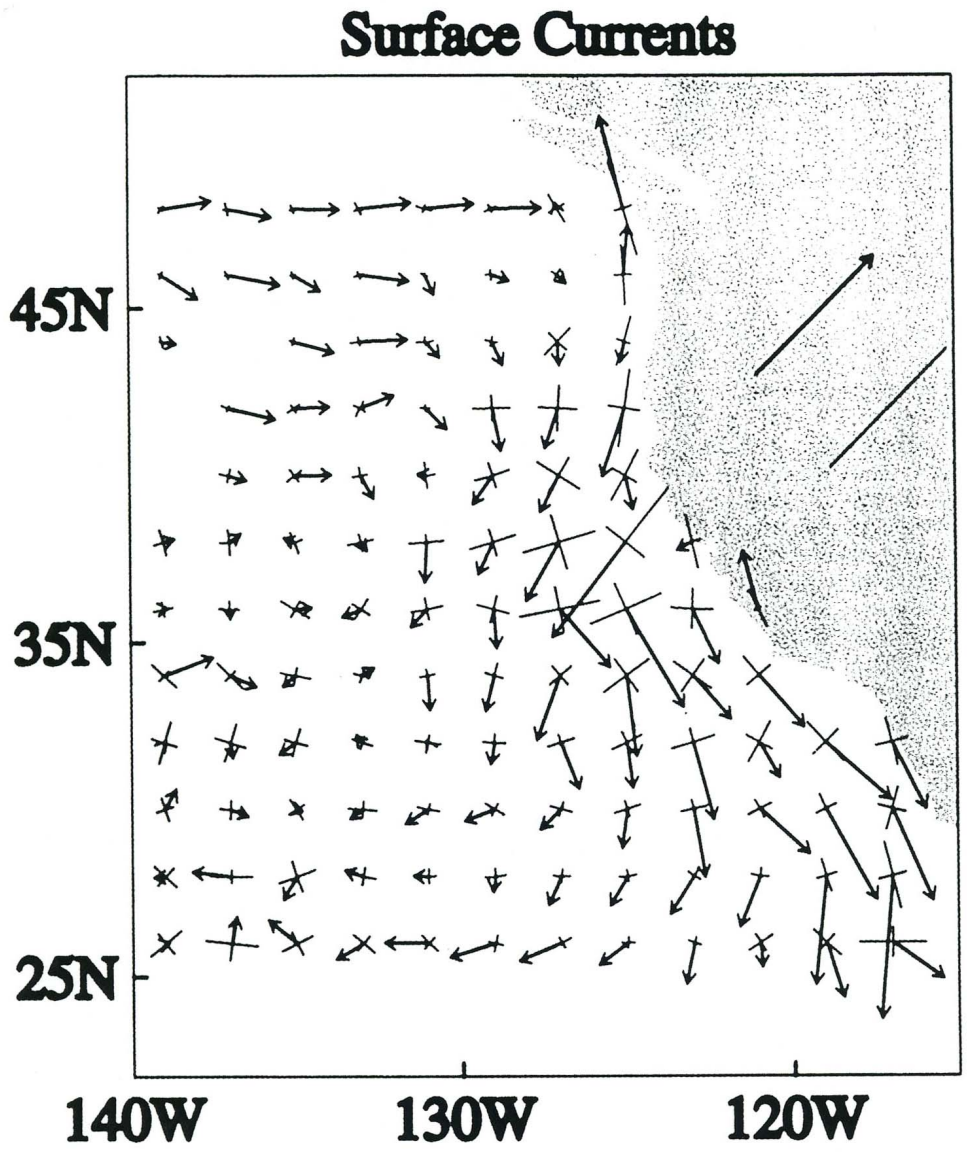

(a) Mean 15-m velocity (reference arrow = 10 cm s^{-1}) and (b) its variance (displayed as major and minor component axes; reference line = 500 cm^2 s^{-2}) in the California Current System (CCS) and eastern Pacific from surface drifters during the period 1985-98. Mesoscale eddies are active in the CCS, generated by baroclinic instability of the alongshore mean flow. (Swenson and Niiler, 1996)

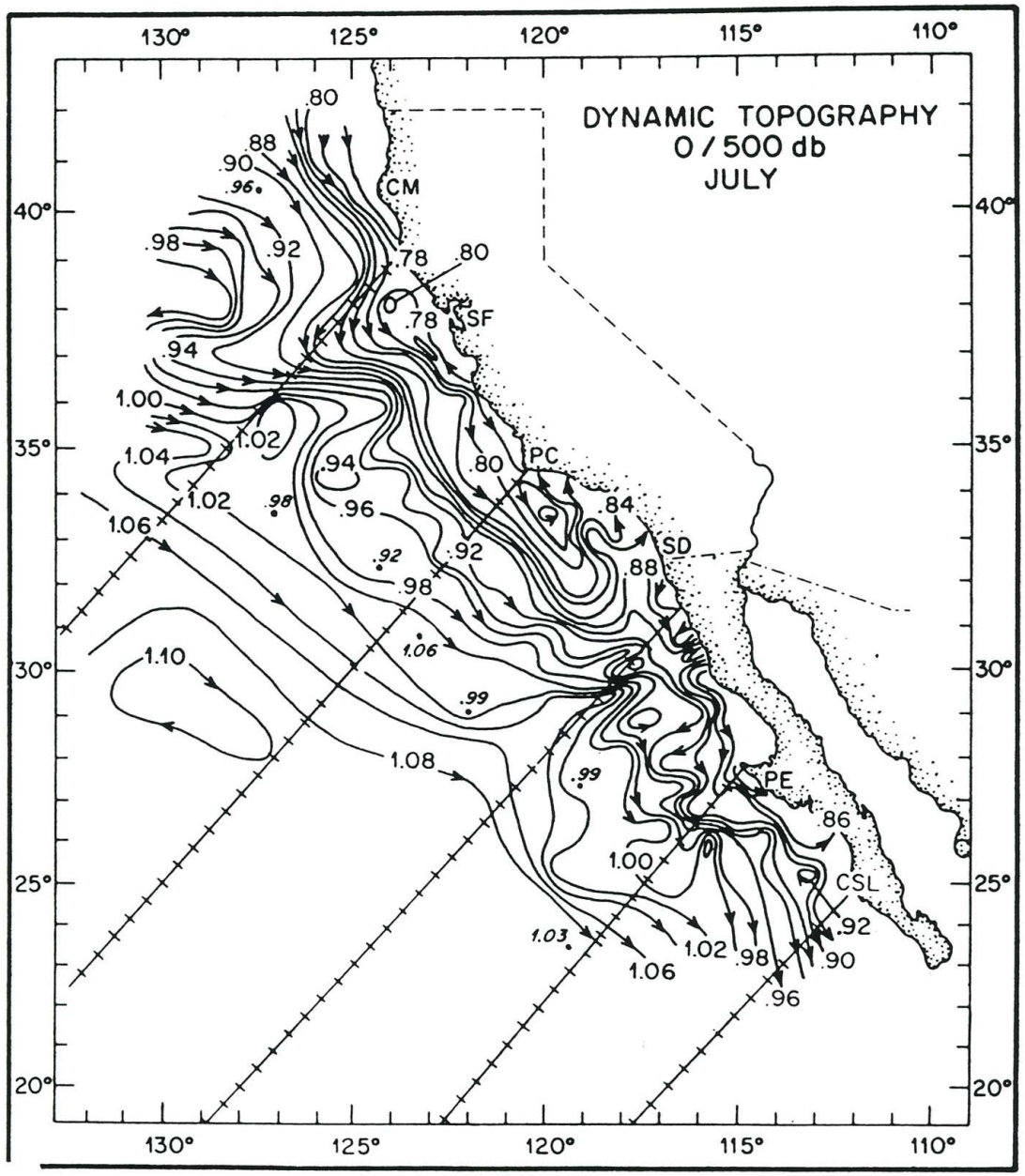

Annual-mean surface dynamic topography ($i.e.$, sea level [m] relative to a sub-thermocline geopotential surface) off the U.S. West Coast (Hickey, 1979). For comparison, $\Delta\eta$ is 10 times bigger across the whole subtropical Pacific or the ACC.

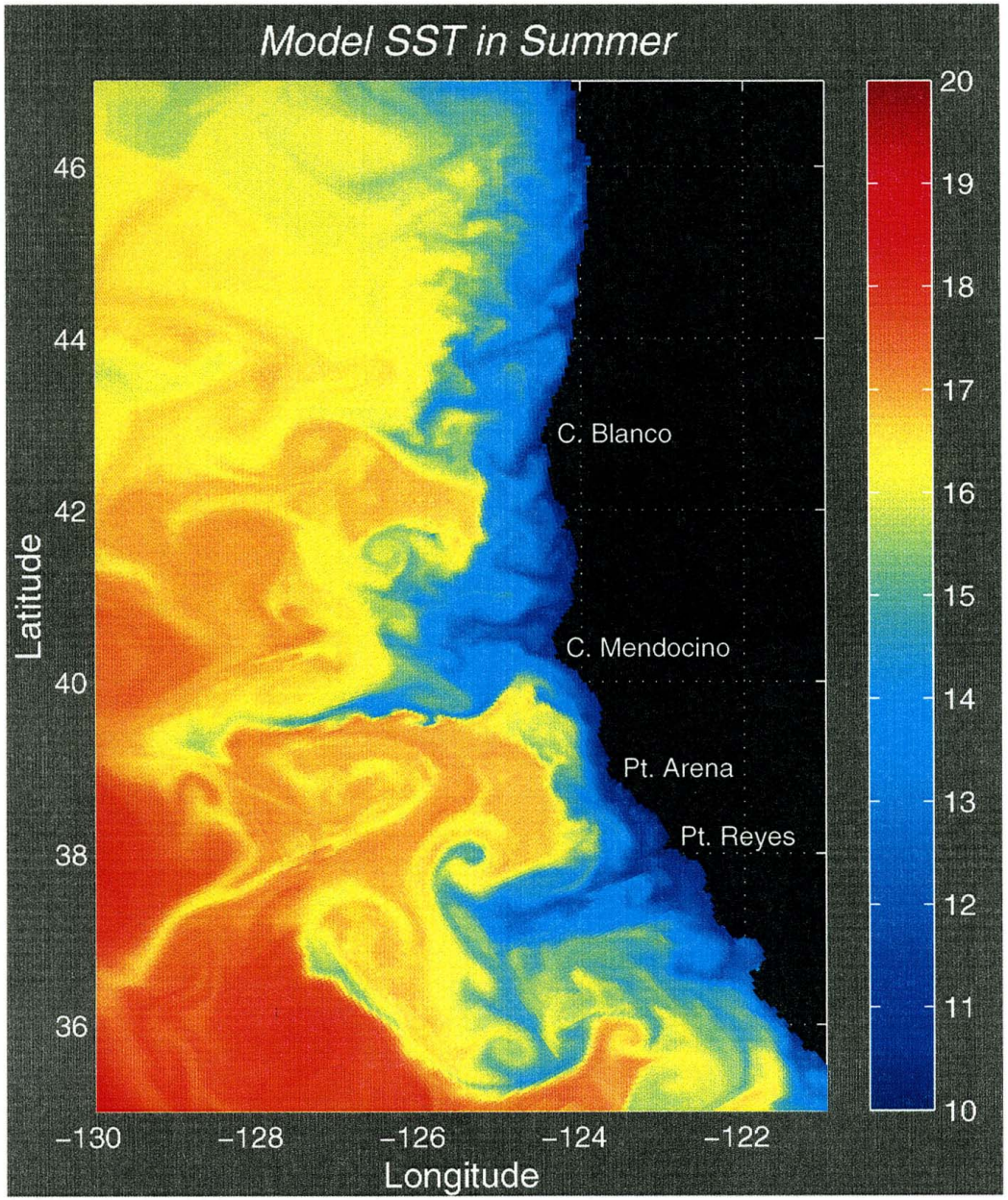

Instantaneous SST [C] in a U.S. West Coast equilibrium model solution. Eddy "squirts and jets" are evident. Plankton blooms and larval dispersal are dominated by eddy flows. (Marchesiello *et al.*, 2003)

Mesoscale Eddy Kinetic Energy

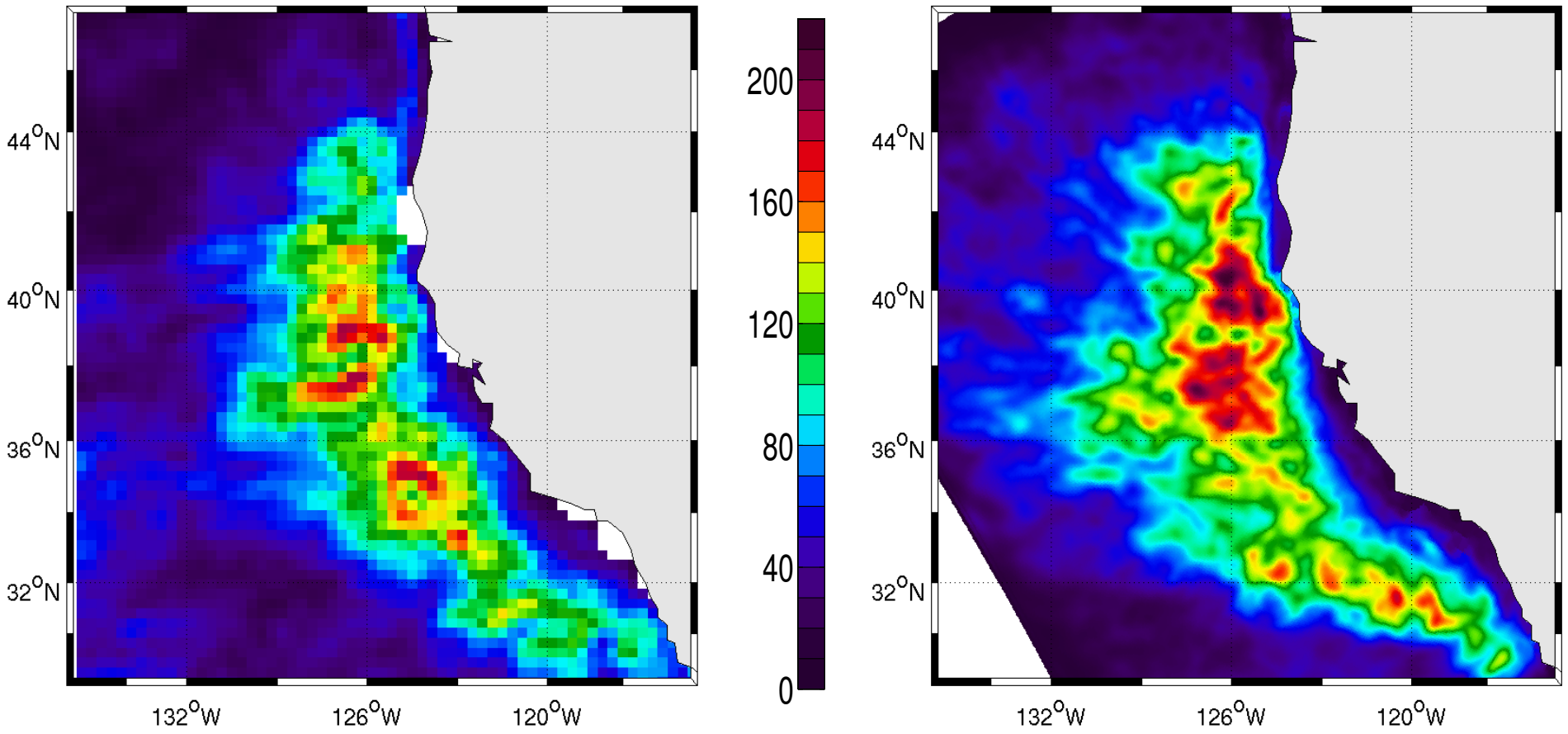

AVISO (altimetry) model

$KE = 0.5 \langle \mathbf{u}'^2 \rangle$ [cm^2 s^{-2}, with peak values around 250].

. . . a sensitive measure of simulation realism.

The estimation uncertainty is substantial for $\sim$ 10-year sample $\pm 30\%$.

Notice the transition around Cape Blanco (43^{o}N) at the edge of the subtropics. (Capet *et al.*, 2008)

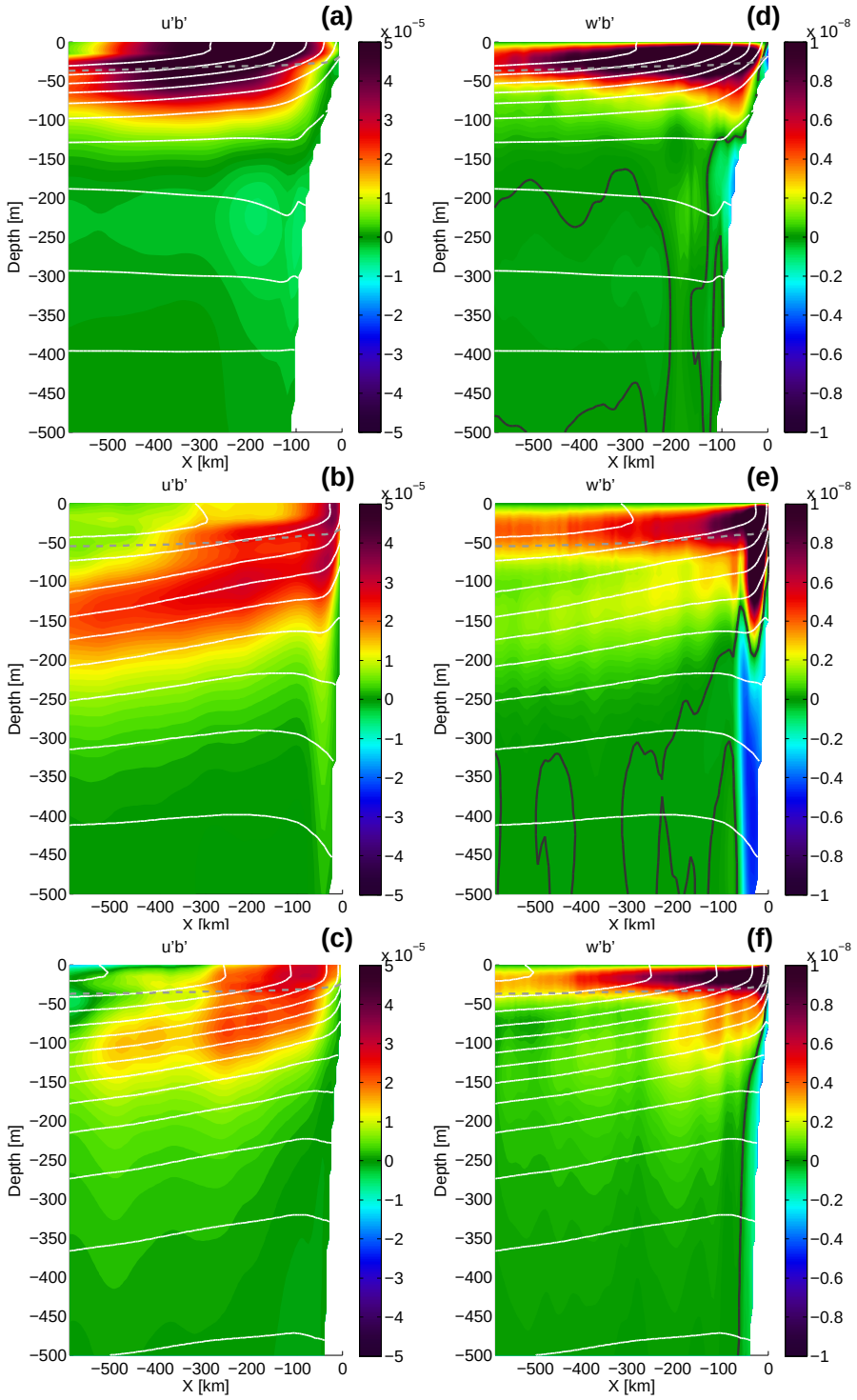

Mesoscale Eddy Buoyancy Flux

Annual along-shore averages of across-shore $\overline{u'b'}$ (left) and vertical $\overline{w'b'}$ (right) eddy buoyancy fluxes $[m^2 s^{-3}]$ for Peru (top), Chile (middle), and California (bottom). White contours are the mean buoyancy field, and the gray dashed line is the mean boundary-layer depth. Black contours are $\overline{w'b'} = 0$. The eddy fluxes are generally shoreward and upward, opposite the mean advection by the zonal upwelling circulation (Colas *et al.*, 2013)

Abyssal Submesoscale Coherent Vortices

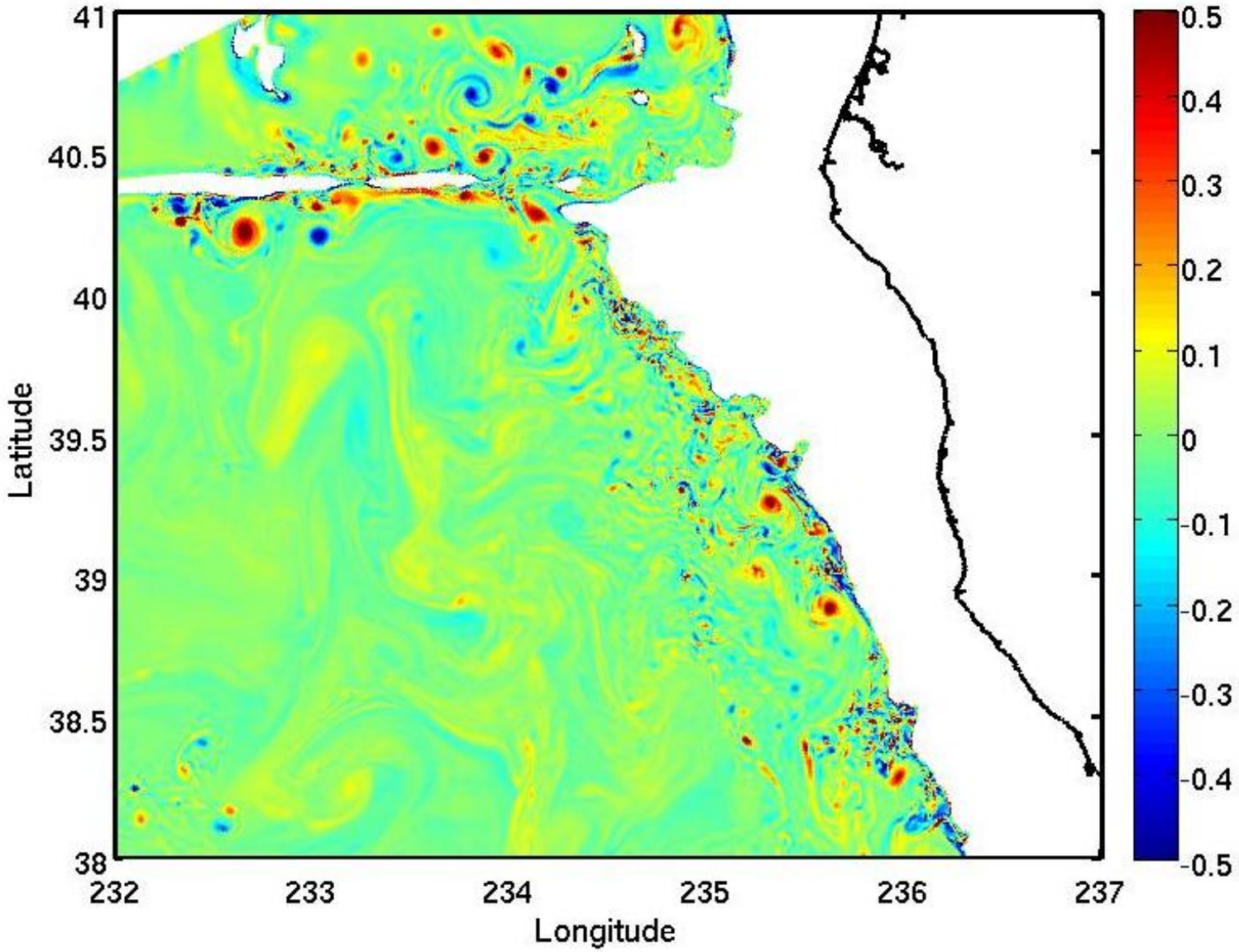

Model simulation of the California Current System: normalized relative vorticity, ζ^z/f, at $z = -2500$ m depth from Pt. Reyes (38^oN) past Cape Mendocino (40.4^oN). These SCVs originate from unstable, separating mesoscale flows along topographic slopes. Current variability is generally larger in coastal zones.

Coastally Trapped Waves

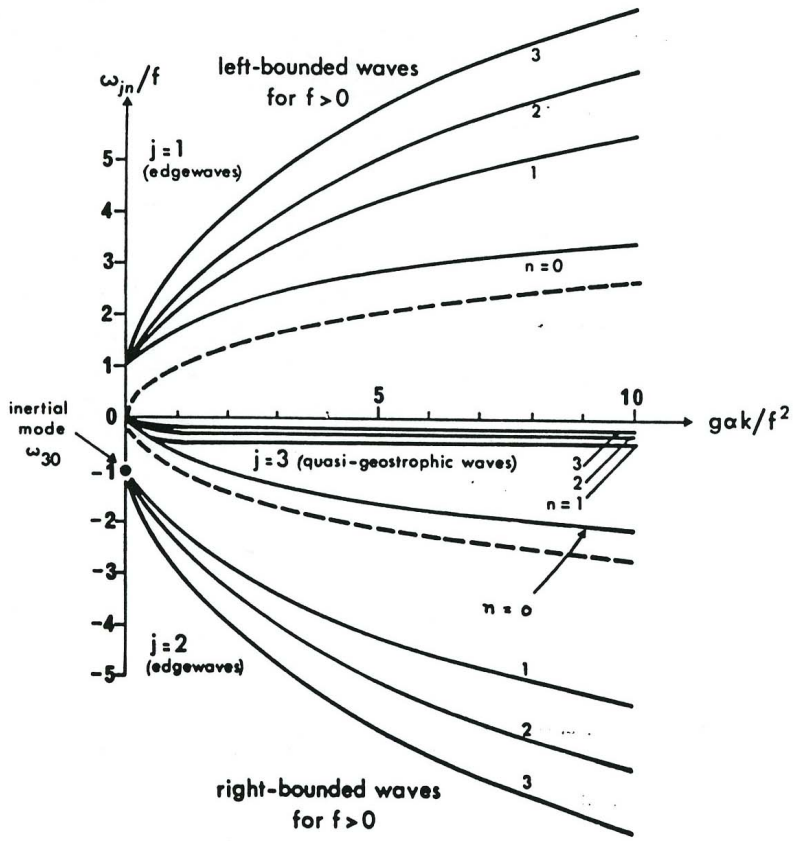

Dispersion relation for waves on a sloping beach. k is alongshore wavenumber. The wave types are gravity edge waves (period $<$ 1 day) and quasigeostrophic topographic waves (periods $\sim$ a few days). The latter propagate with the shore on its right (like a coastal Kelvin wave). They are commonly excited by transient storm winds with similar periods. (LeBlond and Mysak, 1978; Allen, 1980))

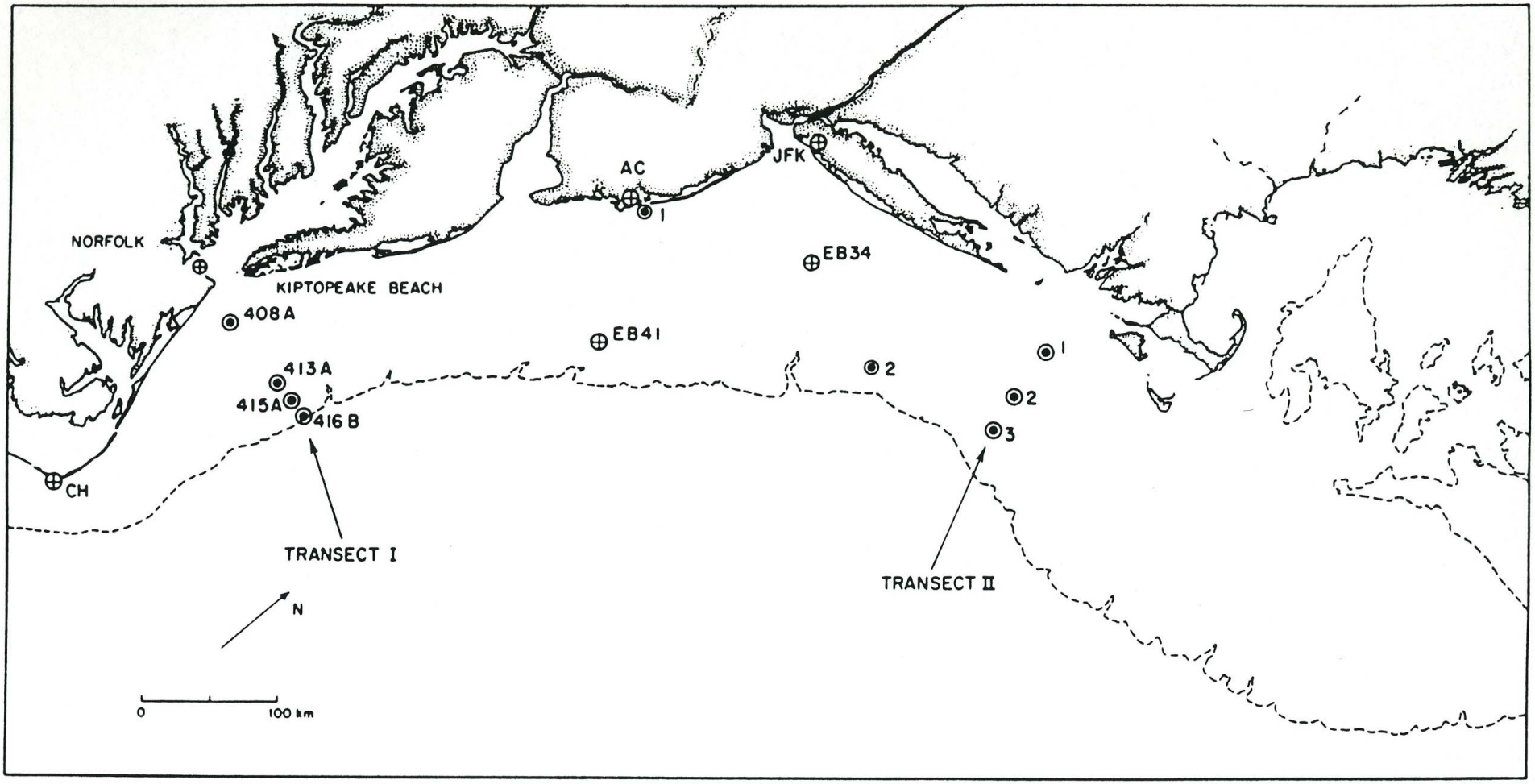

An array of moored wind sensors and current meters on the continental shelf in the Mid-Atlantic Bight off the east coast of the U.S. The dashed line is the shelf break ($i.e.$, edge of the continental slope). It is a wide shelf, and typically it is stratified in summer and well-mixed to the bottom in winter; with corresponding baroclinic and barotropic current structures, respectively. Their data are shown on the next few slides. (Beardsley and Boicourt, 1981)

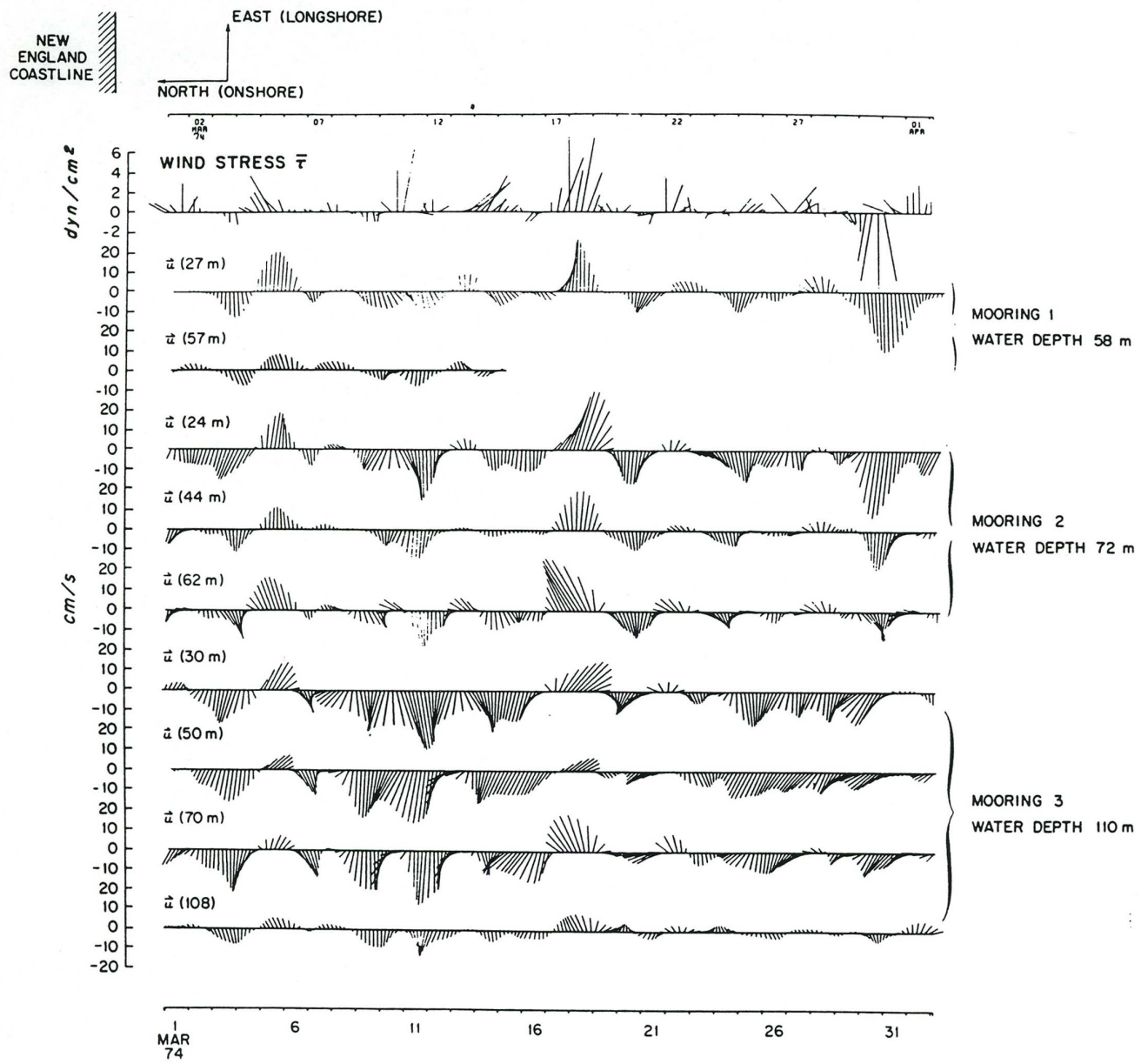

Winter currents along Transect II (slide 15) in the Mid-Atlantic Bight in March, 1974. The sea level and currents mostly vary with storm winds and are a coastally-trapped wave response. They have substantial correlation with depth and alongshore distance. The mean flows are weak (unlike in eastern boundary currents). (Beardsley and Boicourt, 1981)

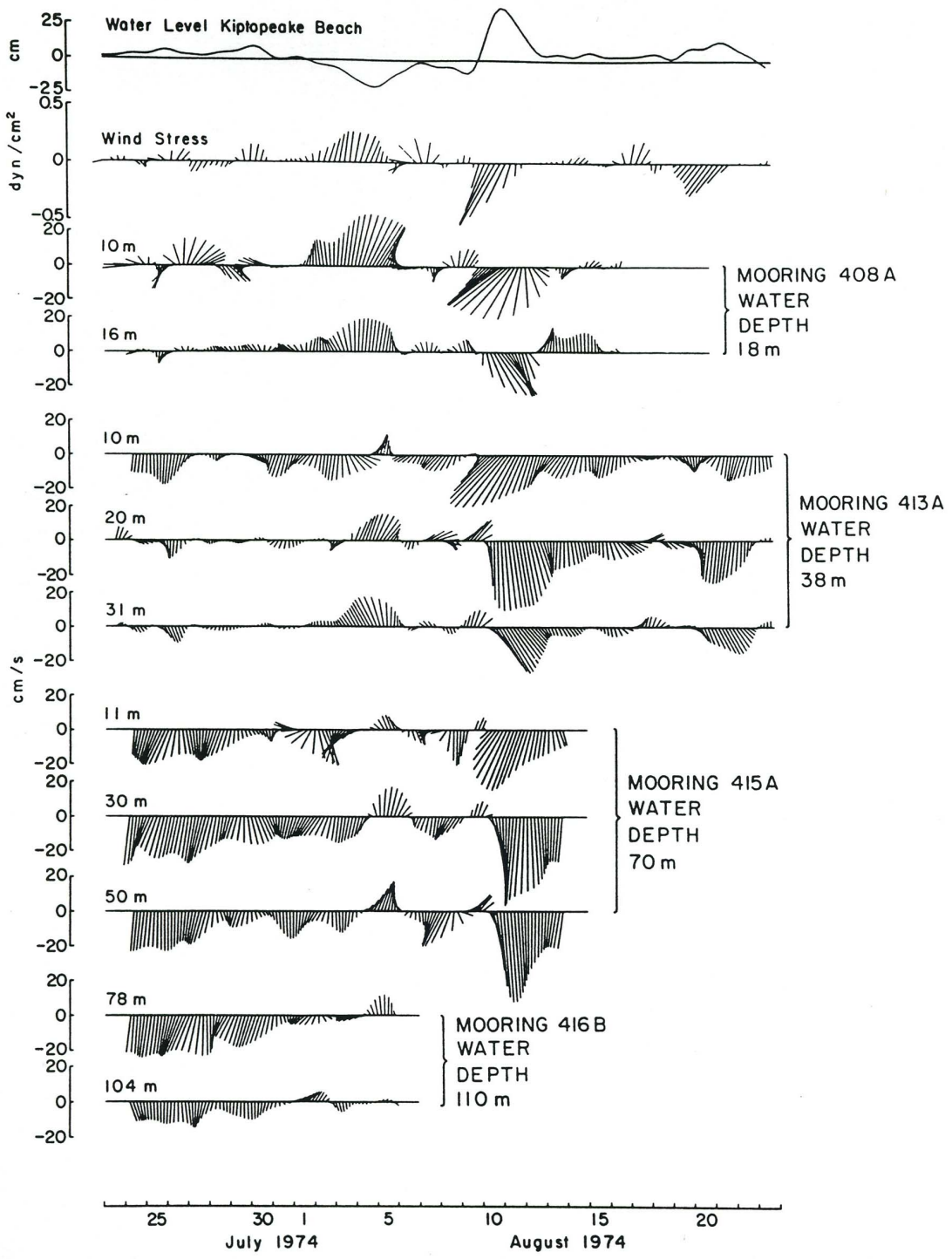

Summer currents in the Mid-Atlantic Bight along Transect I (slide 15) in summer, 1974. Again the main signal is a coastally-trapped wave response. In summer the depth correlation is less, though still significant, because of more stratification, hence a more baroclinic, surface-intensified response. (Beardsley and Boicourt, 1981)

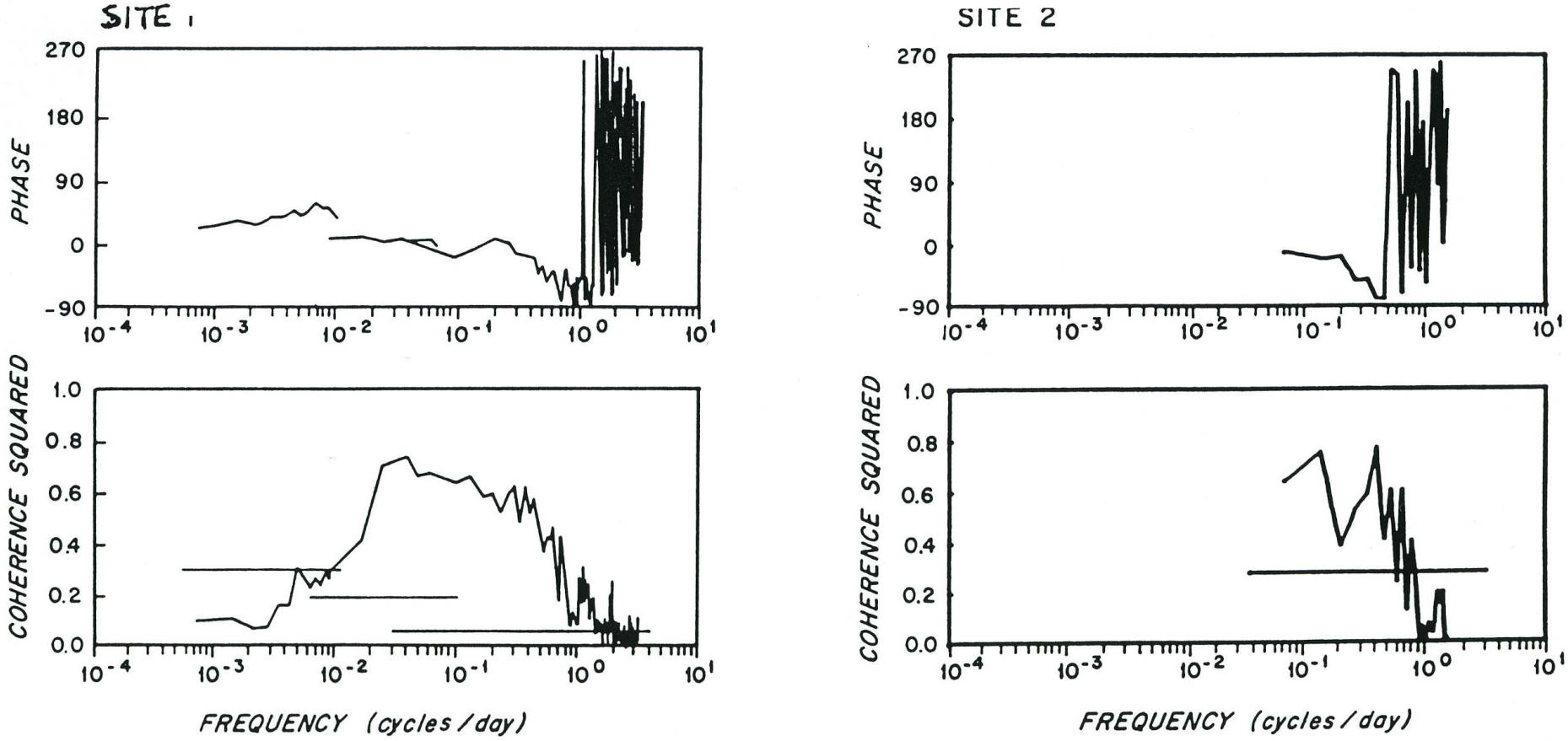

Frequency spectrum correlation analysis (phase and coherence) between local winds and currents at two sites in the Mid-Atlantic Bight. The flat lines indicate levels of statistical significance for the coherence. This shows that the wind and currents are mutually coherent and nearly in phase for frequencies below 1/(2 days). This is consistent with a coastally-trapped wave response. At the lowest frequencies $<$ (1/100 days), the local coherence disappears. (Beardsley and Boicourt, 1981)

Fronts: Mesoscale-Induced

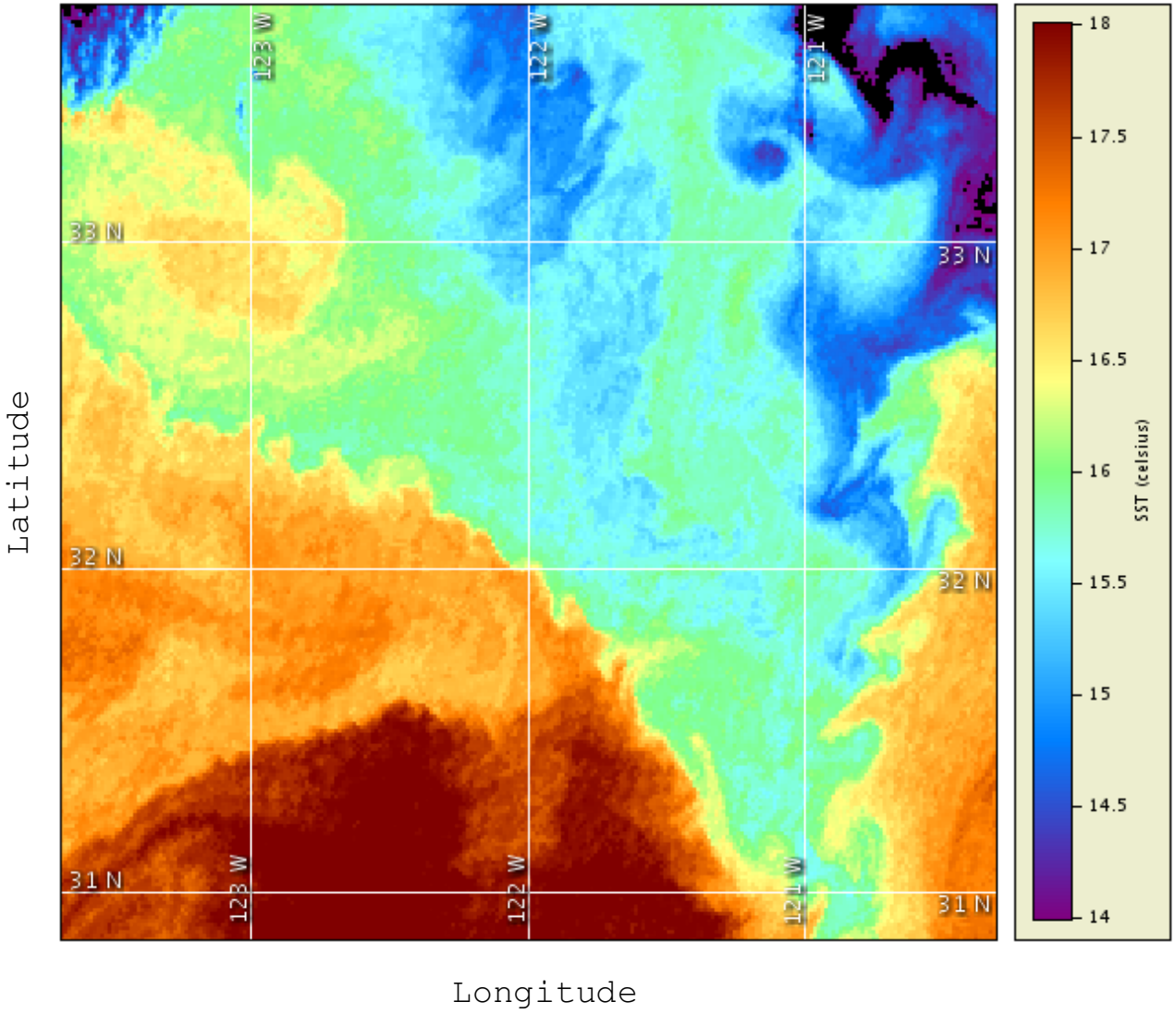

Satellite SST [^{o}C] image off California in $\sim (300\,km)^2$ domain (NOAA COASTWATCH). Notice ~ 100 km mesoscale eddies and ~ 10 km submesoscale fronts with instabilities & vortices. Frontogenesis; "mixed-layer baroclinic", ageostrophic, and centrifugal instabilities of upper ocean currents; and unstable topographic wakes are the primary sources of submesoscale energy. (This is a repeated figure.)

Shelf-Break Fronts

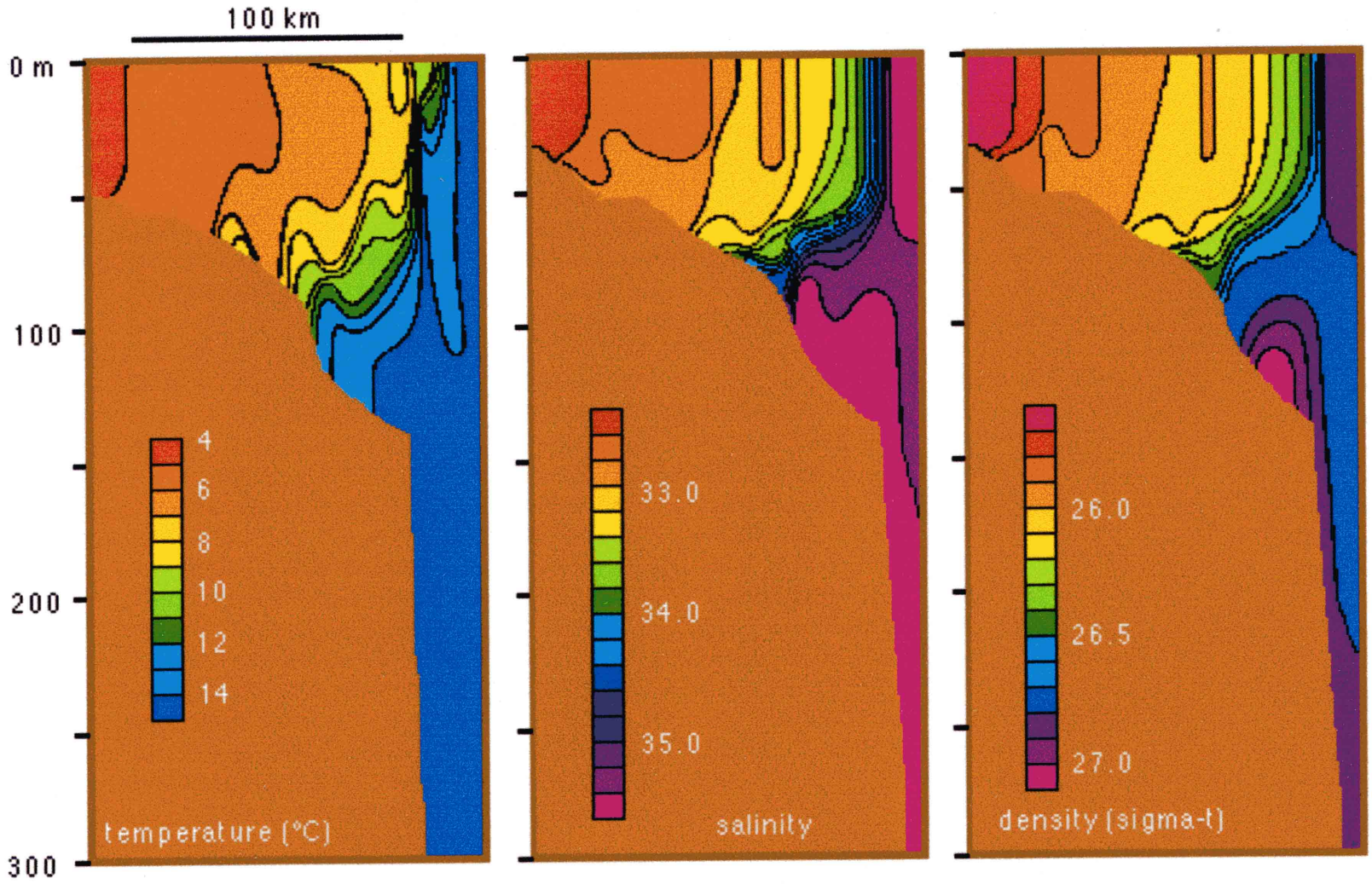

Hydrographic section through the shelf-break front in the Mid-Atlantic Bight, taken south of Rhode Island in April 1974. Winter convective mixing reaches the bottom, and the offshore-flowing bottom Ekman transport of lighter water on a shallow continental shelf often creates a water-mass boundary with the deeper open ocean at the edge of the shelf, where the mixing can no longer reach the deeper bottom because of a stronger thermocline. (Tomczak, 1998; Gawarkiewicz and Chapman, 1992)

Tidal Mixing Fronts

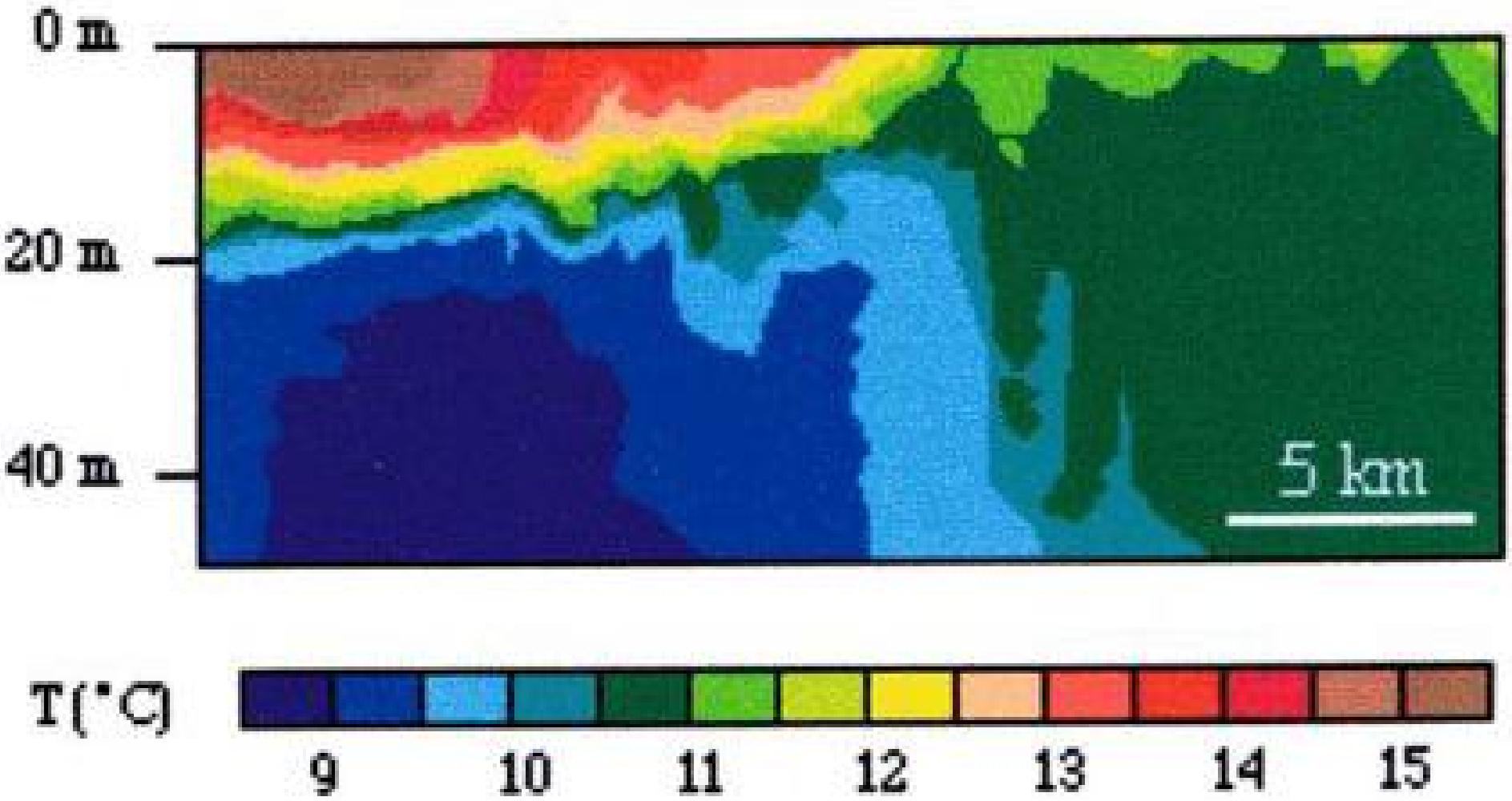

The observed $T(x, z)$ field in a shallow-water front in the Irish Sea where tides are very strong, with deeper water to the left. This example is due to strong tidally-induced vertical mixing where the water is shallow over the continental shelf. (Tomczak, 1998)

Wave-Driven Littoral Currents

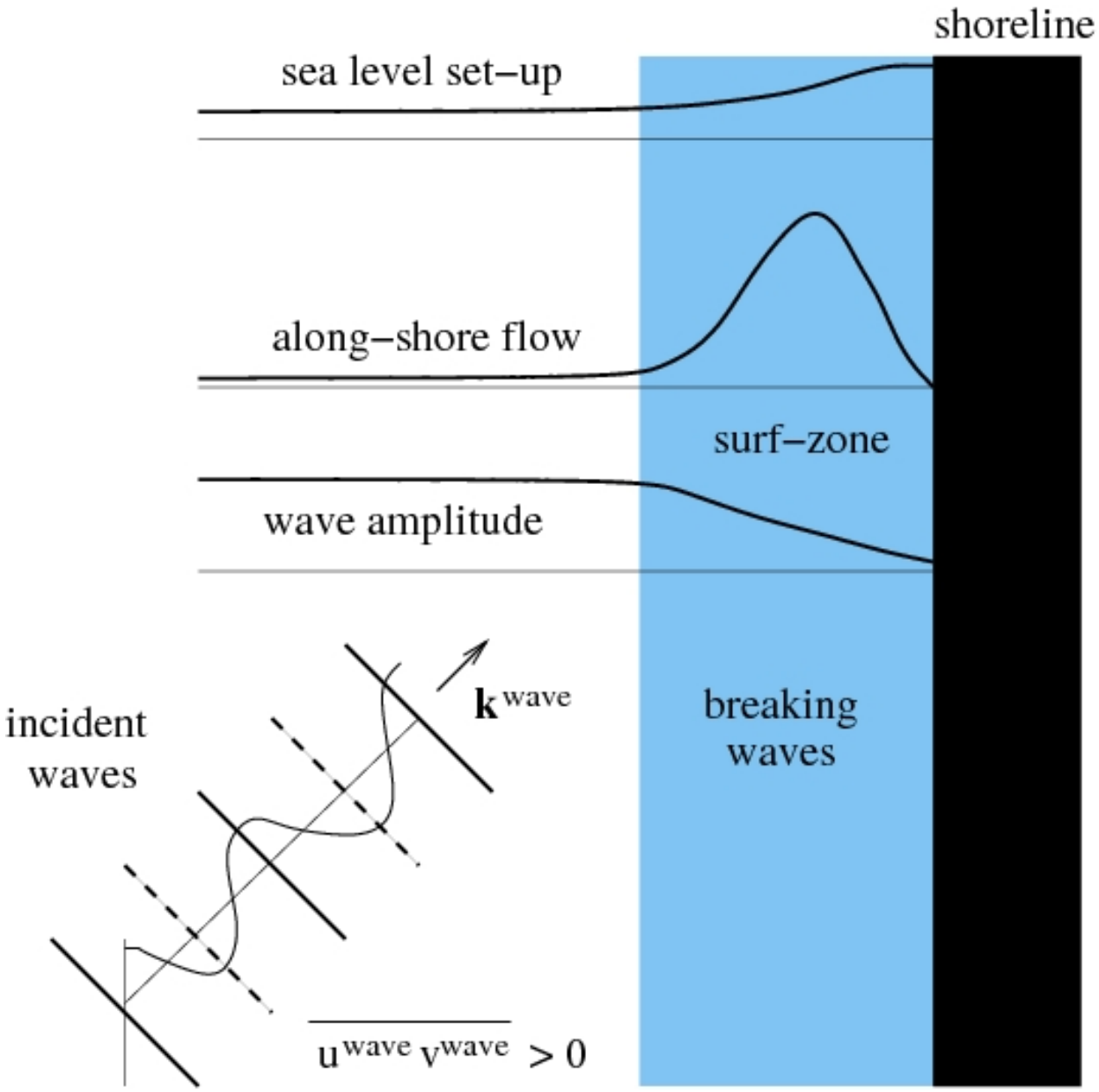

An alongshore littoral current and cross-shore sea-level set-up generated by surf-zone breaking of obliquely incident surface gravity waves; as the waves dissipate near the shore, the along- and cross-shore momentum carried by the offshore wave fields is transfered to the wave-averaged flow and pressure gradients. Further wave effects of currents arise with alongshore non-uniformity, $i.e.$, rip currents with strong offshore surface flow. (Longuet-Higgins, 1970)

Estuarine Circulations

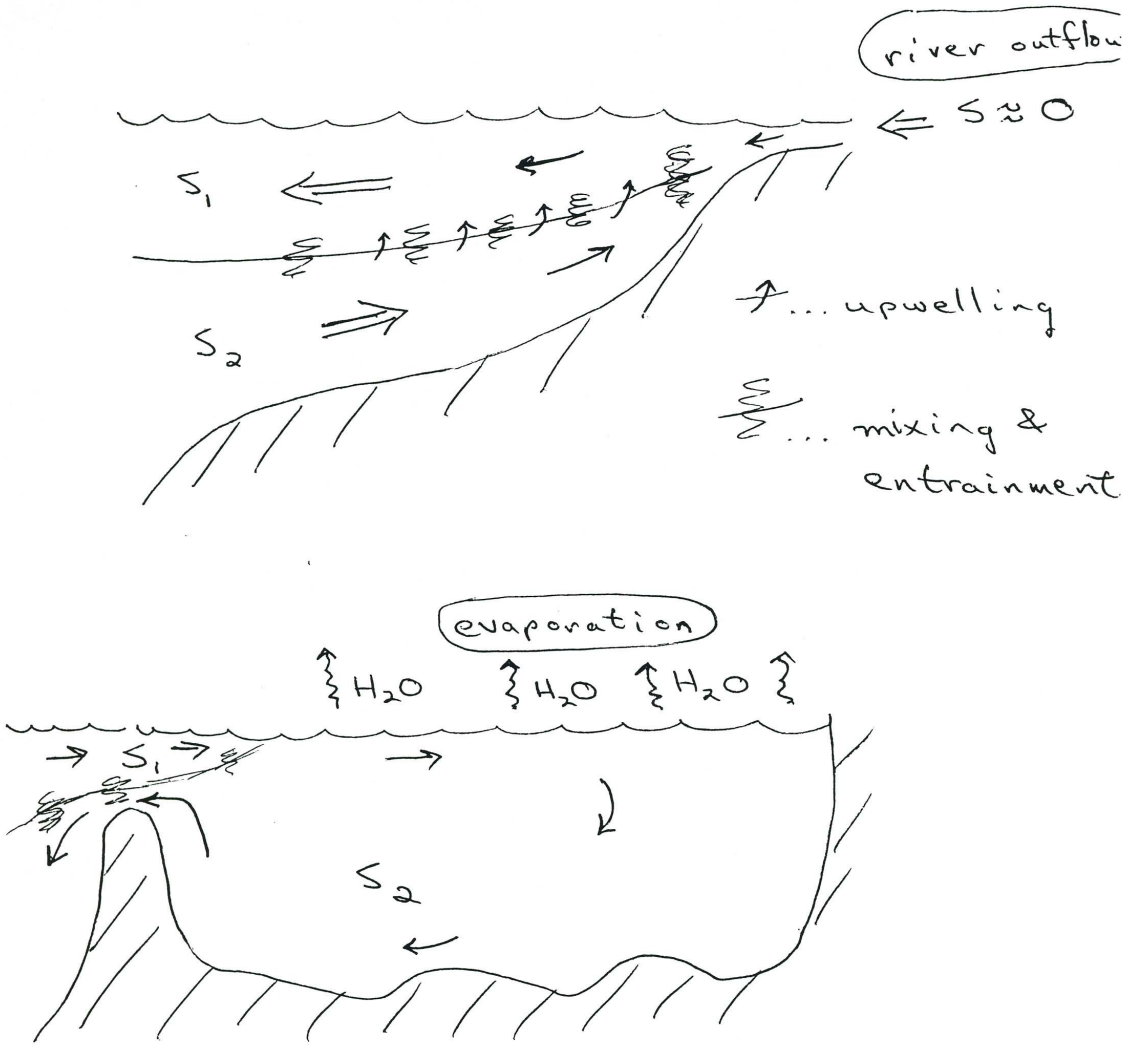

Sketch of estuarine circulations forced by haline gradients with $S_1 < S_2$. The usual situation has shallow fresh water flow into the ocean, but the reverse can happen with excess evaporation in a marginal sea that has a nearly enclosed basin ($e.g.$, Mediterranean Sea).

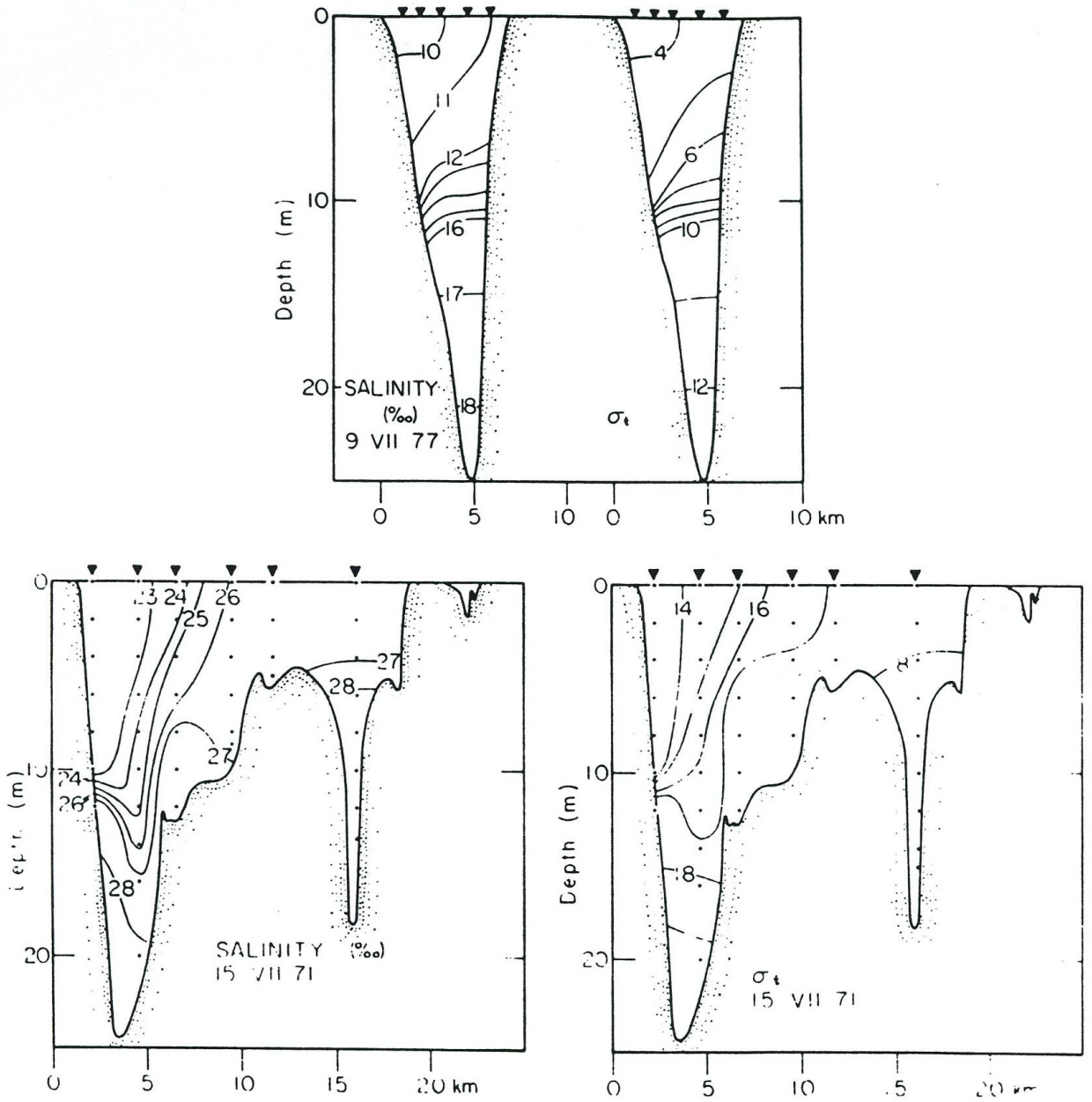

Cross-sections of S [PSU] and $\sigma_t = \sigma_0$ [kg m^{-3}] in Chesapeake Bay: upstream (above) and downstream (below). This is an estuarine flow with fresher water near the surface and upstream. (Beardsley and Boicourt, 1981)

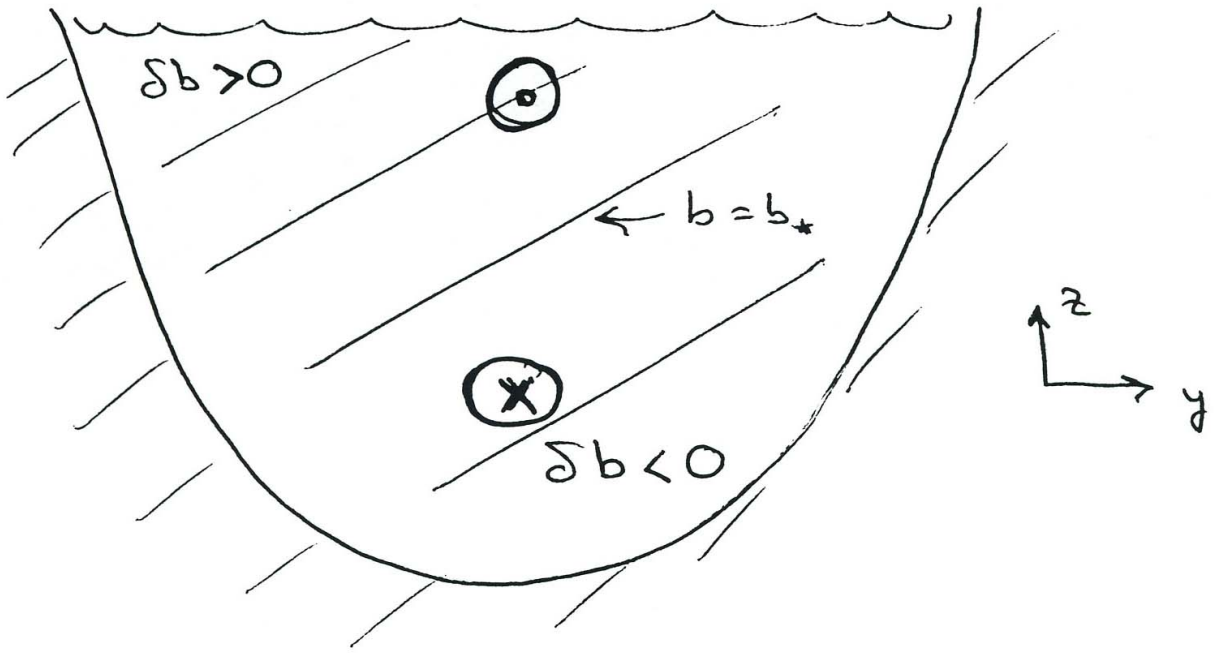

$$u_z = -\frac{1}{f}\phi_{yz}$$

$$= -\frac{1}{f} b_y$$

$$> 0$$

Sketch of isopycnal slopes and currents in Chesapeake Bay. The combination of an estuarine overturning circulation, stable stratification, and geostrophic, hydrostatic balance in a big estuary causes an isopycnal slope across the Bay (*cf.*, slide 23).

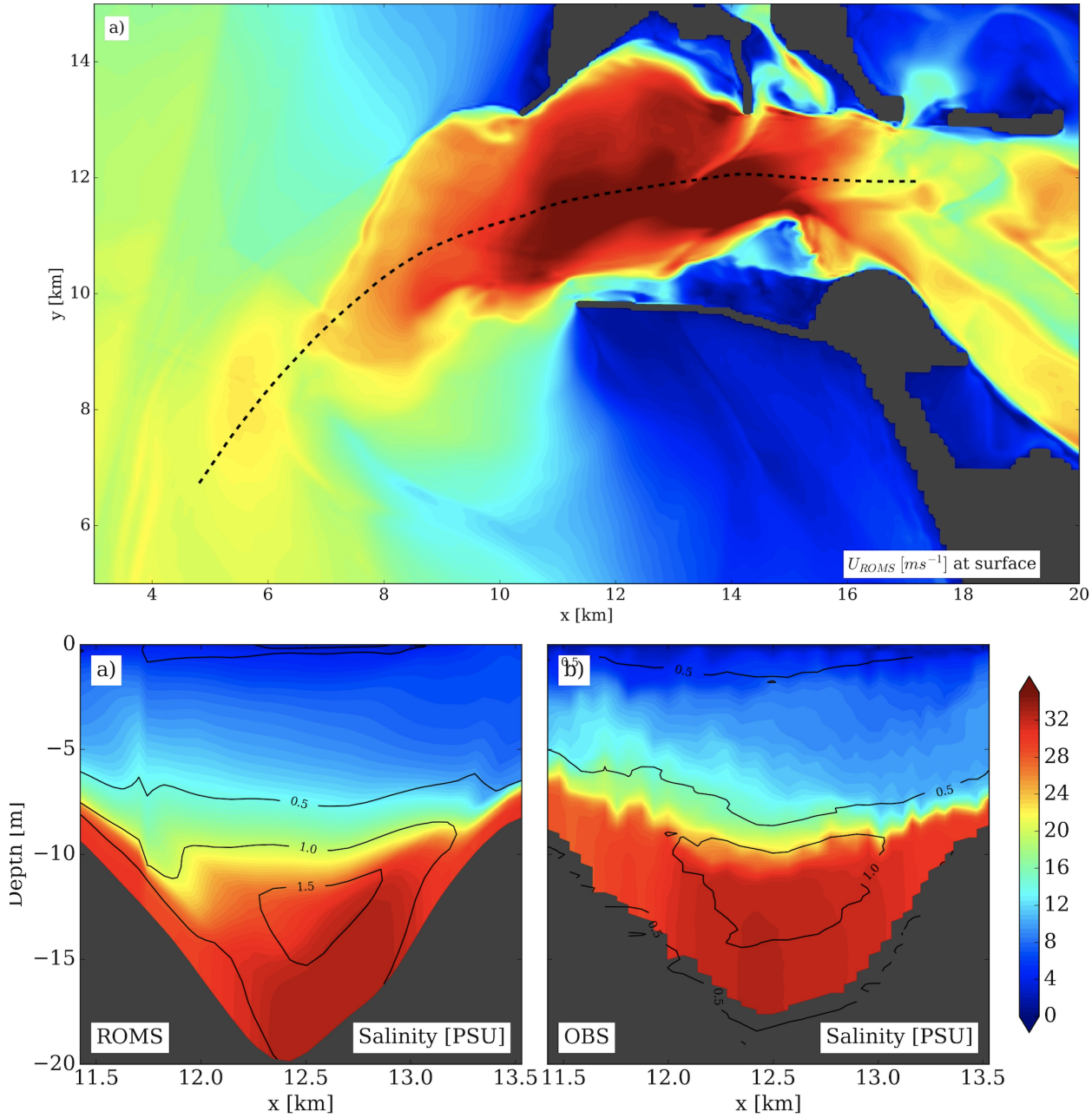

Surface speed [up to 2.5 m/s] (top) and cross-section of Salinity [PSU] (bottom) near the mouth of the Columbia River during peak outflow of a combined river and ebb tide. This is an extreme form of estuarine circulation combined with a river plume during spring run-off. (Akan *et al.*, 2017)

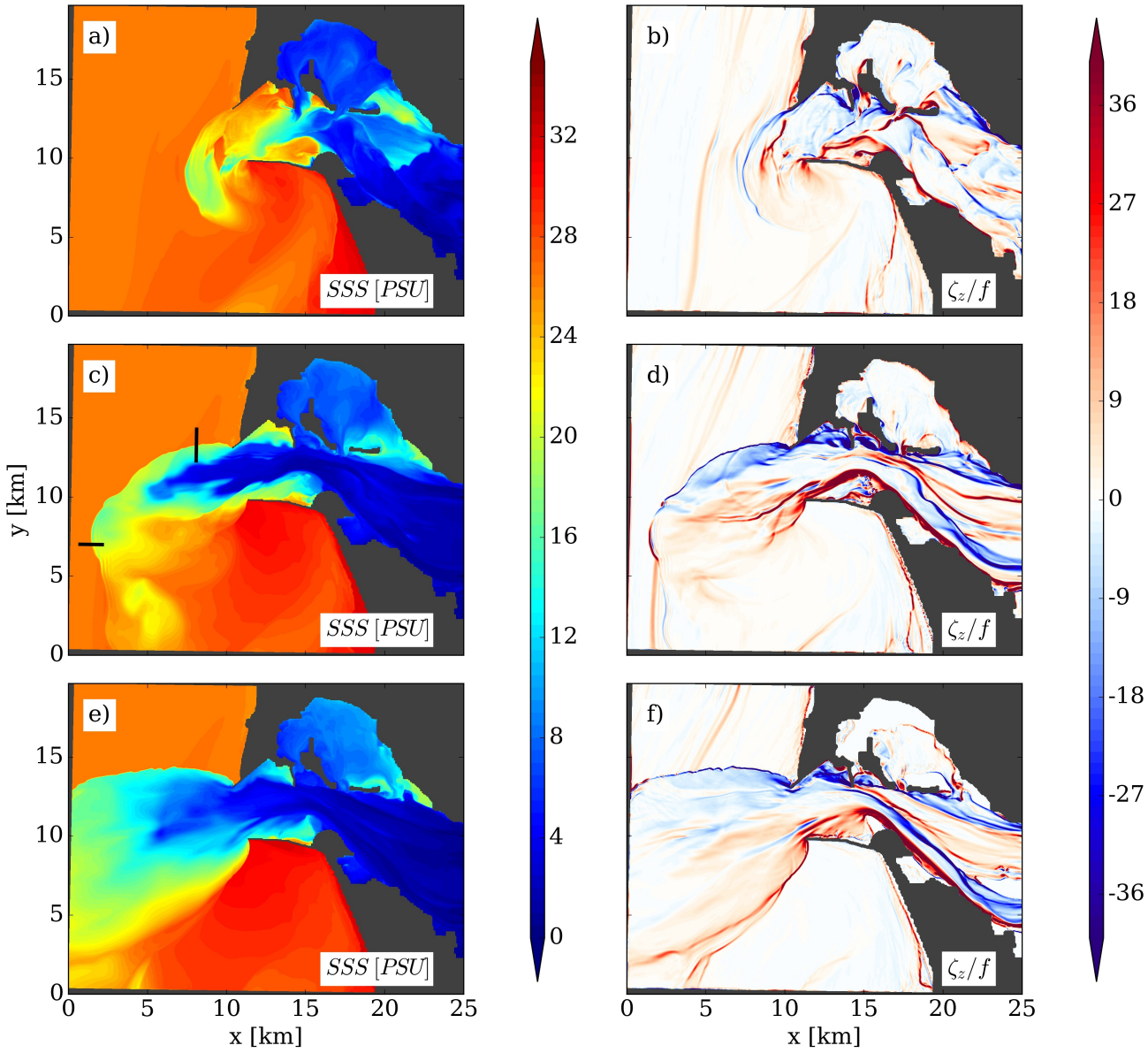

Surface views of the Columbia River plume as it develops during ebb tide: Salinity [PSU] (left) and normalized vertical vorticity ζ^z/f (right). Notice the very sharp leading and side edge fronts; an internal gravity-wave bore and advective frontogenesis, respectively. (Akan *et al.*, 2017)

Coastal Biogeochemistry

Topics that we don't have time to discuss in detail:

- eddy quenching: burial of unconsumed upwelling nutrients by mesoscale eddy mixing on isopycnals descending into the interior, thereby reducing productivity
- river plumes: pollution and eutrophication causing hypoxia and anoxia
- harmful algal blooms, possibly fed by urban wastewater
- swash-zone, intertidal, wetland, and estuarine ecosystems and their land-sea exchanges
- sediment resuspension and transport by waves, tides, and currents ($e.g.$, beach morphological evolution; bioavailable iron release and other sedimentary chemical fluxes)
- larval retention, dispersal, and recruitment for many species
- marine reserves, biodiversity, and bioabundance — refuges from overfishing
- coastal and shoreline fisheries ($e.g.$, shellfish farms imperiled by acidification)

References

Akan, C., J.C. McWilliams, S. Moghimi, and H.T. Ozkan-Haller, 2017: Frontal dynamics at the edge of the Columbia River plume. *Ocean Modelling* **122**, 1-12.

Allen, J., 1980: Models of wind-driven currents on the continental shelf. *Ann. Rev. Fluid Mech.* **12**, 389-433.

Beardsley, R.C., and W.C. Boicourt, 1981: On estuarine and continental-shelf circulation in the Middle Atlantic bight. In: *Evolution of Physical Oceanography*, B.A. Warren and C. Wunsch (eds.), MIT Press, 198-233.

Capet, X., F. Colas, P. Penven, P. Marchesiello, and J.C. McWilliams, 2008: Eddies in eastern-boundary subtropical upwelling systems. In: *Eddy-Resolving Ocean Modeling*, M. Hecht & H. Hasumi, eds., AGU Monograph, 131-147.

Colas, F., X. Capet, J.C. McWilliams, and Z. Li, 2013: Mesoscale eddy buoyancy flux and eddy-induced circulation in eastern-boundary upwelling systems. *J. Phys. Ocean.*, in press.

Gawarkiewicz, G., and D. Chapman, 1992: The role of stratification in the formation and maintenance of shelf break fronts. *J. Phys. Ocean.* **15**, 713-748.

Hickey, B.M., 1979: The California current system—hypotheses and facts. *Prog. Ocean.* **8**, 191-279.

LeBlond, P., and L. Mysak, 1978: *Waves in the Ocean*. Elsevier Press, 602 p.

Longuet-Higgins, M.S., 1970: Longshore currents generated by obliquely incident sea waves. *J. Geophys. Res.* **75**, 6778-6801.

Marchesiello, P., J.C. McWilliams, and A. Shchepetkin, 2001: Open boundary conditions for long-term integration of regional ocean models. *Ocean Modelling*, in press.

O'Brien, J.J., 1975: Models of coastal upwelling. In: *Numerical Models of Ocean Circulation*, R.O. Reid (ed.), Nat. Acad. Sci. Press, 204-215.

Les guides du SHOM, La Mare, 1997, Ref. OG941.

Stewart, Robert, 2008: *Introduction to Physical Oceanography.*
`http://oceanworld.tamu.edu/resources/ocng_textbook/PDF_files/book_pdf_files.html`

Swenson, M.S., and P.P. Niiler, 1996: Statistical analysis of the surface circulation of the California Current. *J. Geophys. Res.* **101**, 22631-22645.

Tomczak, M., 1998: *Shelf and Coastal Oceangraphy.*
`http://gyre.umeoce.maine.edu/physicalocean/Tomczak/ShelfCoast/index.html`